Original Paper

Effects of lamp alignment and downward (minus) tilting of mirror-lamp systems on the growth of Pr-doped $Lu_3Al_5O_{12}$ crystals by floating zone method

Md. Zahid HASAN[1], Naoki NODA[1], Satoshi WATAUCHI[1*], Yuki MARUYAMA[1], Masanori NAGAO[1], Shunsuke KUROSAWA[2,3], Yuui YOKOTA[4], Akira YOSHIKAWA[2,4,5], Koichi KAKIMOTO[6], Isao TANAKA[1]

[1]Center for Crystal Science and Technology, University of Yamanashi, 7-32 Miyamae, Kofu, Yamanashi 400-0021
[2]New Industry Creation Hatchery Center (NICHe), Tohoku University, 6-6-10 Aoba, Aramaki, Aoba-ku, Sendai, Miyagi 980-8579
[3]Department of Physics, Yamagata University, 1-4-12 Kojirakawa-machi, Yamagata 990-8560
[4]Institute for Materials Research, Tohoku University, 2-1-1 Katahira, Aoba-ku, Sendai, Miyagi 980-8577
[5]C&A Corporation, 1-15-9 Ichibancho, Aoba-ku, Sendai, Miyagi, 980-0811
[6]Research Institute for Applied Mechanics, Kyushu University, 6-1 Kasuga-koen, Kasuga, Fukuoka, 816-8580

Received April 7, 2021; E-mail: watauchi@yamanashi.ac.jp

We explored conditions for the growth of Pr-doped $Lu_3Al_5O_{12}$ (Pr:LuAG) single crystals using the infrared convergent floating zone (IR-FZ) method. We newly examined the effects of the lamp alignment, and downward (minus) tilting of the mirror-lamp (M-L) systems because the grown crystals were opaque and contained numerous cracks in the conventional growth conditions. In the conditions, a highly concave melt-crystal interface was observed during crystal growth and a ring crack was recognized at the core region in a cross section of a grown crystal. The formation of the ring crack was found to be closely related with the highly concave melt-crystal interface. However, downward (minus) tilting of the M-L systems facilitated obtaining a slightly concave melt-crystal interface and suppressing the ring crack. Further efforts are required to obtain a crack-free Pr:LuAG crystal.

Key Words: *Floating zone, Interface, Lamp alignment, Tilt of mirror-lamp system*

1. Introduction

Scintillation materials are used widely in the field of high energy physics, medical imaging such as computed tomography (CT), and positron emission tomography (PET) [1-4]. These materials are also used for natural resource exploration, magneto-optics, and characterization of laser and optical materials [5]. Praseodymium-doped $Lu_3Al_5O_{12}$ (Pr:LuAG) is known as an inorganic scintillator for X-ray or γ–ray, with a high light yield of approximately 19,000 photon/MeV, density of 6.63 gm/cm^3, and excellent energy resolution of 4.6%@662 keV [6]. In addition, it is non-hygroscopic in nature.

Pr:LuAG crystals have already been grown by various methods, such as the Czochralski method (CZ) [7,8], vertical Bridgman method [9], and micro-pulling-down method [7] because LuAG is a congruent melting compound [10]. The melting temperature of LuAG is 2060 °C. The crystals grown by these methods show significant segregation of Pr. Although a large crystal of Pr:LuAG, 92 mm in diameter, can be grown by the CZ method, the solidification fraction has to be extremely limited [8]. As crucibles made of iridium (Ir) are necessary for crystal growth employing these methods, the manufacturing cost of such crystals could be affected by the price of Ir.

Therefore, control of the segregation and development of a crucible-free growth method is desirable in crystal growth of Pr:LuAG. From this point of view, the infrared heating floating zone method (IR-FZ) is promising, as it is a crucible-free zone melting crystal growth method [11]. The segregation of the dopant can be controlled by using a solvent with appropriate composition. In the IR-FZ method, the molten zone is maintained at a position between a feed rod and grown crystal without a crucible. The molten zone is controlled by the balances between the gravity and surface tension of the melt. For successful growth, it is essential to maintain a stable molten zone during crystal growth. The typical size of the crystal grown by this method is limited to 6–15 mm in diameter [11]. It is difficult to maintain a stable molten zone when growing a crystal with larger diameter is attempted [12-14].

Some co-authors of this paper have managed to improve the diameters of grown crystals of rutile and silicon even in the IR-FZ method by changing the convergent conditions [14-17]. By controlling the convex melt-crystal interface shape by upward (plus) tilting of the mirror-lamp (M-L) systems and stabilizing the molten zone by the tilt, larger crystals of rutile and silicon could be grown. The diameters achieved were 19 mm for rutile and 45 mm for silicon.

In the present study, we attempted to optimize the growth conditions of Pr:LuAG crystals by employing the IR-FZ method because the grown crystals were opaque and contained numerous cracks in the conventional growth conditions. A highly concave melt-crystal interface was also observed during crystal growth. Therefore, we newly examined the effects of vertical alignment of the lamps and the downward (minus) tilting effect of the M-L systems on crystal growth of Pr:LuAG by the IR-FZ method. These effects on the molten zone shape will be discussed by introducing the parameters characterizing molten zone shape during the crystal growth.

2. Experimental

High-purity Pr_6O_{11} (99.99%), Lu_2O_3 (99.99%), and α-Al_2O_3 (99.99%) were used as starting materials for feed preparation. In our experiment, the nominal composition formula was $(Pr_{0.01}Lu_{0.99})_3Al_5O_{12}$. The appropriate amount of powder was mixed

with ethanol using a mortar and a pestle. The powder mixture was calcined at 1,200 °C for 12 h in air and heated again at 1,450 °C for 12 h in air after dry mixing. To form a rod shape, the fine powder was put into a rubber tube and pressed up to 300 MPa by a hydrostatic pressuring machine (Nikkiso Co. Ltd., Japan, Model CL3-22-60) after sealing the rubber tube. The pressed feed rods were subsequently sintered at 1,500 °C for 5 h in air. The typical size of the sintered rod was 9–11 mm in diameter and 50–70 mm in length. A modified infrared convergent heating image furnace (model FZ-T-10000-H-TY-1: Crystal Systems Corporation, Japan), with four-ellipsoidal mirrors and four halogen lamps, was used for crystal growth. A summary of the main growth conditions is presented in Table I.

Fig.1 shows our experimental setups for the effects of the vertical lamp alignment and the downward (minus) tilting on the growth of Pr:LuAG crystals. In the conventional IR-FZ method, the alignments of the halogen lamps are horizontal, as shown in Fig.1(a), and the tilting angle (θ) is zero. The definition of the θ is shown in Fig.1(b). In this conventional lamp alignment, a rather narrow temperature distribution was expected that could lead to significant thermal shock. On the other hand, in the vertical alignment, a rather wide temperature distribution was expected that could reduce the thermal shock. In the current experiment, both alignments were applied for crystal growth of Pr:LuAG. Fig.1(b) shows a schematic illustration of downward (minus) tilting of the M-L systems. In the present furnace, the θ could be changed from 0° to -10°. The dashed lines of each ellipsoidal mirror show the parts of the mirror that were scraped off to realize downward (minus) tilting. In this experiment, tilting angles of both 0° and -10° were applied to observe the downward (minus) tilting effects clearly. Some of the grown crystals were cut along the perpendicular to the growth direction to observe the cut surface. The orientations of a few grains were checked by the back-reflection Laue X-ray diffraction (XRD).

Table I Typical growth conditions for Pr:LuAG crystals

Total rated lamp output (kW)	10
Lamp alignment	Horizontal, Vertical
Tilting angle θ (°)	0, -10
Feed diameter (mm)	9–11
Rotation rate (upper/lower) (rpm)	3/40
Moving rate (upper/lower) (mm/h)	7.5/5.0
Growth atmosphere	Ar, 200 mL/min

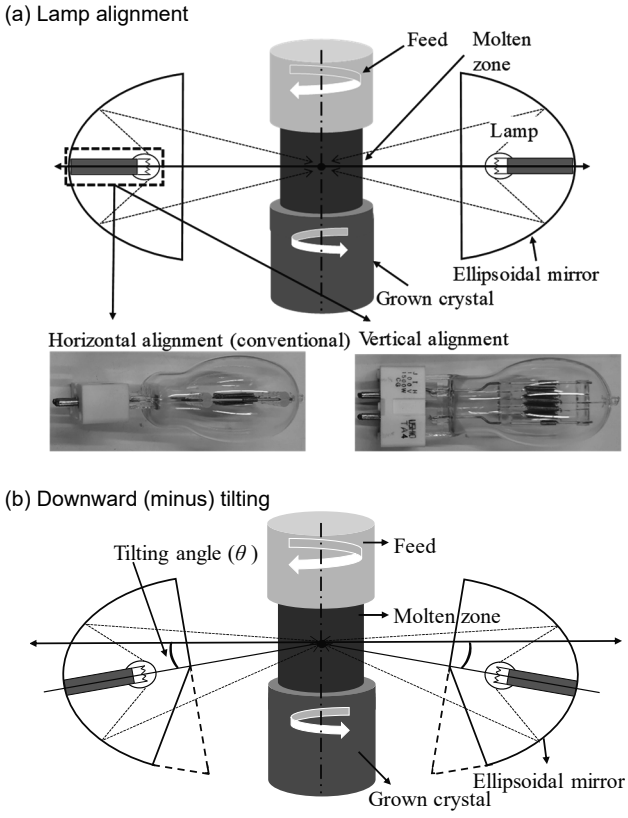

Fig.1 Schematic illustration of the experimental setup for (a) the lamp alignment and (b) the downward (minus) tilting of the M-L systems.

To observe the solid-liquid interface carefully, the molten zone during crytal growth was quenched by turning off the heating lamps quickly after stopping the rotations of both the upper and lower shaft. The quenched samples were cut along the growth direction at the center and polished to a mirror-like surface. The parameters characterizing the interface shape were directly determined from the photographs of the quenched molten zone obtained during crystal growth.

3. Results and Discussion

Fig.2(a)–(c) shows the 1.0 at% Pr-doped LuAG crystals grown under various conditions. Fig.2 (a) shows the crystal grown in the horizontal alignment of lamps and the non-tilted configuration of the M-L systems, the so-called conventional condition. The grown crystal contained numerous cracks and it was opaque, particularly in the latter part of the grown crystals. Although Kitamura *et al*, reported that the use of the heat reservoir was quite effective to suppress the crack formation of $Y_3Al_5O_{12}$ crystal grown by the IR-FZ [19], it was difficult to melt Pr:LuAG under the condition of using a heat reservoir in our furnace. Fig.2(b) and (c) shows the crystal grown in vertical lamp alignment and the crystal grown in the downward (minus) tilted condition of the M-L systems, respectively. Although quantitative evaluations are difficult, the opacity of the grown crystal was improved in these crystals. Also shown in Fig.2

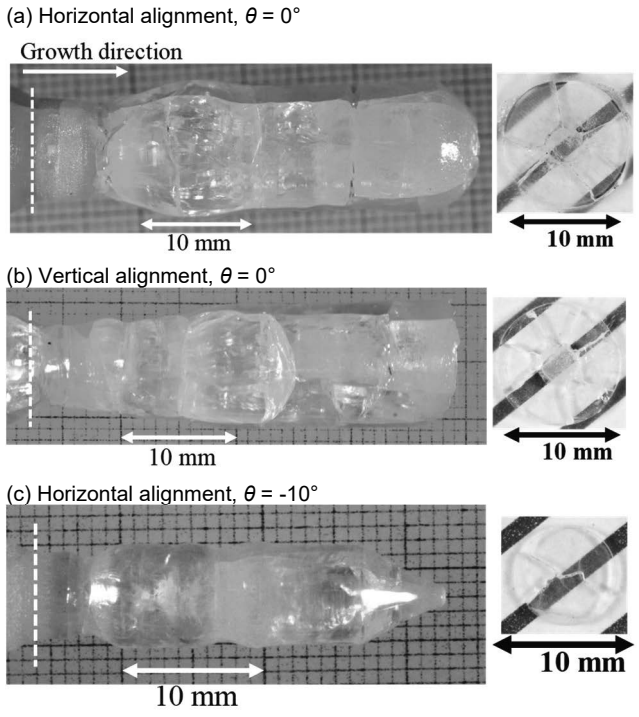

Fig.2 1.0 at% Pr-doped LuAG crystals grown under various conditions. (a) Non-tilted horizontal lamp alignment; (b) Non-tilted vertical lamp alignment; (c) Downward (minus) tilted horizontal lamp alignment.

(a), (b), and (c), are the disk-like crystals sliced perpendicular to the growth direction. A ring crack and some radial cracks were observed in the core area and the peripherical area, respectively, as shown in Fig.2(a) and (b). The core area was opaquer than the peripherical area. Only radial cracks were observed, as shown in Fig.2(c). In Fig.2(c), the number of radial cracks was also reduced.

Fig.3(a) and (b) shows Laue X-ray diffraction images observed on the various surface positions of the sliced samples of the crystals of Fig.2(a) and (c). The crystallographic orientations were found to be the same not only in the same grains but also in the adjacent grains. These results suggest that cracks were formed during the cooling process.

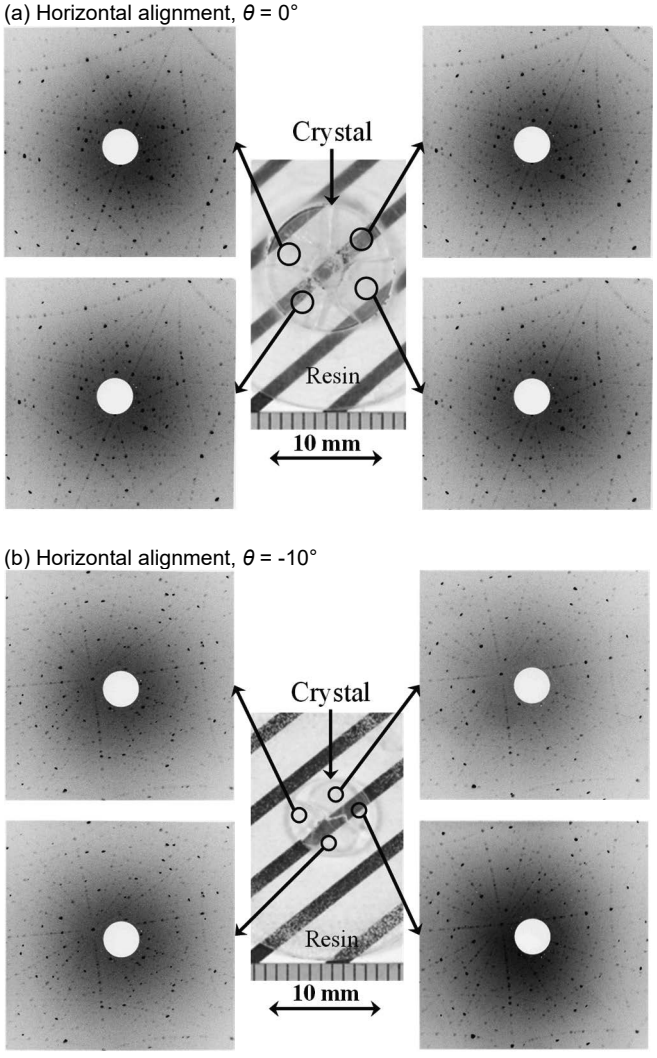

Fig.3 Laue X-ray diffraction images observed on the various surface positions of the sliced samples of the crystals grown in (a) the non-tilted condition and (b) the downward (minus) tilted condition.

Fig.4(a), (b) and (c) shows images of molten zone area during crystal growth under various convergent conditions in (a) horizontal lamp alignment and non-tilted conditions, (b) vertical lamp alignment and non-tilted conditions, and (c) horizontal lamp alignment and downward (minus) tilted conditions. The molten zones were stable and the cracks appeared free in the grown crystals just below the molten zone. However, the grown crystals contained cracks at room temperature, as shown in Fig.2(a), (b) and (c). Therefore, some of the cracks were expected be formed during the cooling process. In Fig.4, λ, *L*, and *L`* are also defined as the penetration depth of the melt toward the feed rod, zone length at the peripherical area and zone length at the core area of the molten zone.

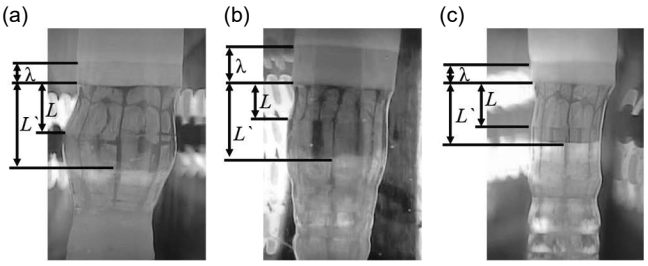

Fig.4 Images of molten zone area during crystal growth under various convergent conditions in (a) horizontal lamp alignment and non-tilted conditions, (b) vertical lamp alignment and non-tilted conditions, and (c) horizontal lamp alignment and downward (minus) tilted conditions. λ, L, and L` show the penetration depth of the melt toward the feed rod, zone length at the peripherical area, and the zone length at the core area of the molten zone.

A qualitative discussion of the temperature gradient can be conducted on the behaviors of λs, which are expected to be independent of the feed diameter. Larger values of λs suggest less temperature gradient around the molten zone area. As shown in Fig.4, λ of Fig.4(b) was longer than the others, suggesting that the temperature gradient around the molten zone area was gentler than the others. In the vertical lamp alignment, the convergent area was expected to be longer along the vertical direction compared with that in the horizontal alignment. The observed behaviors of λs were consistent with this scenario. λ shown in Fig.4(c) did not differ much from that shown in Fig.4(a), suggesting that the temperature gradient in the feed-melt interface was not affected by the downward (minus) tilting of the M-L systems compared with the vertical lamp alignment.

For all conditions in Fig.4, each *L`* was longer than each *L*, implying that the melt-crystal interfaces were concave toward the grown crystal. Concave melt-crystal interfaces have been reported that often cause the formation of cracks in a grown crystal, as well as inclusions at the core area of a grown crystal [19-21]. All our grown crystals contained numerous cracks, probably caused by the concave melt-crystal interface. *L`-L* was longer in the vertical lamp alignment [Fig.4(b)] and shorter in the downward (minus) tilted condition of the M-L systems [Fig.4(c)] compared with the conventional conditions of the horizontal lamp alignment and the non-tilted configuration of the M-L systems [Fig.4(a)]. These results imply a highly concave interface [Fig.4(b)] and a less concave interface [Fig.4(c)], respectively, although the interface shapes could be affected by the grown crystal diameter and the applied lamp power [12,16,22]. As we mentioned above, in the vertical lamp

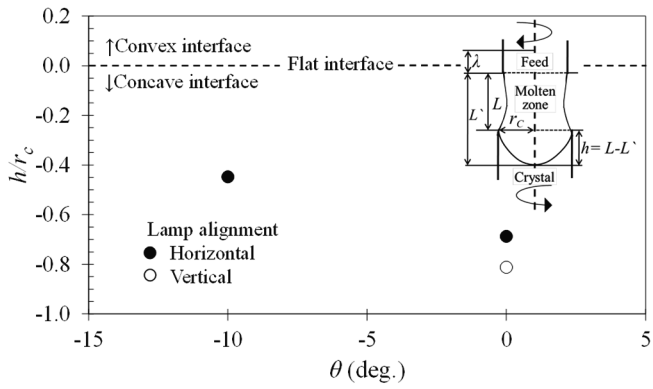

Fig.5 θ dependencies of h/r_C observed in the image of the molten zone during the crystal growth. Inset: Schematic illustration for defining parameters characterizing the molten zone shape.

alignment, the convergent area was expected to be longer along the vertical direction compared with that in the horizontal alignment. The less temperature gradient may be realized around the molten zone area, which is responsible for the highly concave interface in Fig.4(b). The ring crack observed in Fig.2(a) and (b) was not observed in Fig.2(c), which could be attributed to a less concave interface [Fig.4(c)].

As shown in the inset of Fig.5, we defined r_c and h to discuss the molten zone shape quantitatively. The values of the h were negative because the values of L` were bigger than those of L as shown in Fig.4. Fig.5 shows h/r_c as a function of θ because h can be affected by the diameter of the grown crystals. The values of h/r_c were negative, which means that the melt-crystal interfaces were concave for both the non-tilted and the downward (minus) tilted conditions. If the melt-crystal interface was flat or convex, the value of h/r_c should be zero or positive, which is consistent with the values of convexity discussed in refs. [12, 15-18, 22]. The value of h/r_c was -0.68 for the non-tilted condition (θ = 0°), which changed to -0.45 in the downward tilted condition (θ = -10°). A highly concave interface was changed to a slightly concave interface by the downward (minus) tilting. Although the ring crack was observed in the core area of the crystal grown under the highly concave interface as shown in Fig.2(a) and (b), it was suppressed in the crystal grown under the slightly concave interface as shown in Fig.2(c). Thermal stress in a grown crystal can be released in slightly concave interface.

Fig.6 shows that the images of the quenched sample around the convergent heated area sliced along the growth direction. The highly concave melt-crystal interface and the slightly concave interface were clearly recognized for the non-tilted condition and for the tilted condition, respectively. As shown in Fig.6(a), the formation of a ring crack, which was closely related with the bending of the melt-crystal interface, was also recognized in the grown crystal. Some stress can be concentrated in the bending position. Neither a ring crack in the grown crystal nor the bending of the crystal-melt interface were recognized in Fig.6(b). Therefore, a highly concave crystal-melt interface must cause the difficulty of crystal growth by the IR-FZ method. A concave melt-crystal interface also means that the temperature at the peripherical area is lower than that at the central area in the same horizontal level around the melt-crystal interface region. Our experimental results indicate that the downward (minus) tilt is effective to heat the peripherical area preferentially. In such a sense, a more downward (minus) tilting of the M-L systems should be applied to realize the flat or convex interface shape, which could not be done owing to the limit of our image furnace.

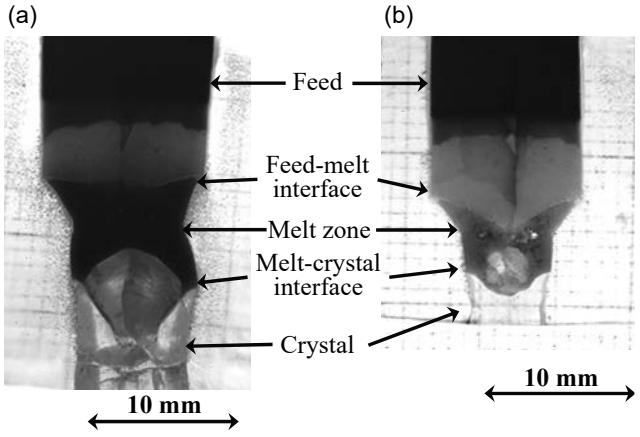

Fig.6 Quenched samples around the convergent heated area sliced along the growth direction. (a) θ = 0°, (b) θ = -10°.

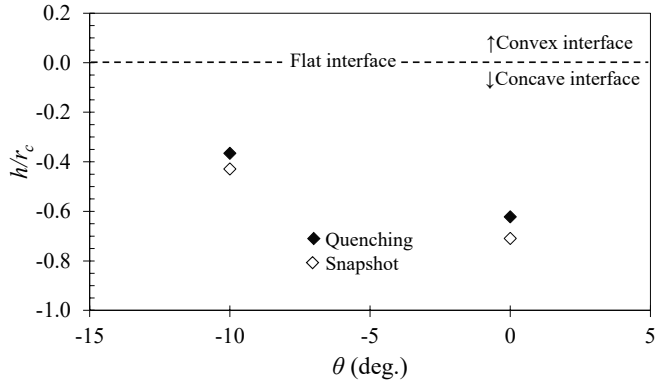

Fig.7 θ dependencies of h/r_C for the quenched samples.

Fig.7 shows h/r_c as the function of θ for the quenched samples. The values of h/r_c determined by both the images of the molten zone are during the growth like Fig.4 and the images of the sliced samples as shown in Fig.6 were compared. Although the absolute values of h/r_c were slightly different between the molten zone image and the quenched sample, the behaviors of h/r_c were consistent, which means that the behavior of h/r_c can be discussed simply by the images like Fig.4. The value of h/r_c for the grown-crystal side increased from -0.62 to -0.36 with the decrease of θ from 0° to -10° based on the quenched samples. This behavior was similar with the behavior of h/r_c of the interface of the molten zone during rutile growth. In the growth of a rutile crystal, the value of h/r_c for the grown-crystal side increased from 0.19 to 0.55 with the decrease of θ from 20° to 0° [15, 17].

Fig.8 shows the schematic illustration of the mirror-tilting effects at θ = 0° (a) and -10° (b). The highly concave melt-crystal interface was changed to the slightly concave interface by the downward (minus) tilting of the M-L systems. These observed behaviors can be explained by the change of the radiation condition. The concave interface means the temperature of the peripherical area is lower than that of the core area in the same horizontal plane around convergent region. In the downward tilted condition, the peripherical area of the grown crystal is expected to be heated more widely than the core area, which can reduce the temperature difference between the peripherical area and the core area in the same horizontal plane. Although the change of the convection flow caused by the tilting also can affect the molten zone shape, it is hard to be discussed. For further discussions, the simulation study on the melt convection and on the temperature distribution in the molten zone are important.

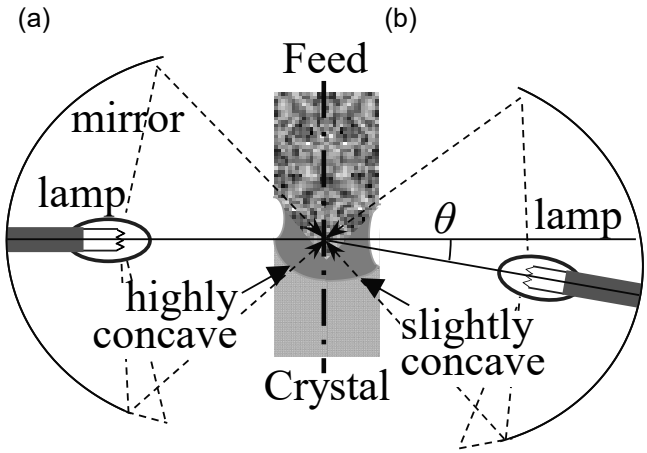

Fig.8 Schematic illustration of mirror tilting effects on the interface shapes. (a) θ = 0°, (b)θ = -10°.

4. Conclusions

We studied the effects of the lamp alignment, and downward (minus) tilting of the M-L systems on the growth of Pr:LuAG crystals by the floating zone method using infrared convergent heating. However, the grown crystals were opaque and contained numerous cracks in the conventional convergent conditions. The presence of a highly concave melt-crystal interface was also observed. It was found that the downward (minus) tilting of the M-L systems was useful to realize the slightly concave interface and to suppress the ring crack at core region of the grown crystal. The radial cracks were also reduced.

Acknowledgement

This work was partially supported by the GIMRT Program of the Institute for Materials Research, Tohoku University and by the RIAM Program of the Research Institute for Applied Mechanics, Kyushu University. We would like to thank Editage (www.editage.com) for English language editing.

References

1) W. W. Moses, *Phys. Res. B.,* **2002**, *487*, 123.
2) M. M. Ter-Pogossian, *Diagnostic Imaging in Medicine*, Edited by Reba RC, Goodenough DJ, Davidson HF., Springer (Netherlands), **1983**, 273.
3) H. Schöder, Y. E. Erdi, S. M. Larson, H. W. Yeung, *Eur. J. Nucl. Med. Mol. Imaging.*, **2003**, *30*, 1419.
4) M. Nikl, A. Yoshikawa, *Adv. Opt. Mater.*, **2015**, *3*, 463.
5) Z. Hu, M. Cao, H. Chen, Y. Shi, H. Kou, T. Xie, L. Wu, Y. Pan, X. Feng, A. Vedda, A. Beitlerova, M. Nikl, J. Li, *Opt. Mater.*, **2017**, *72*, 201.
6) W. Drozdowski, P. Dorenbos, J. T. M. de Haas, R. Drozdowska, A. Owens, K. Kamada, K. Tsutsumi, Y. Usuki, T. Yanagida, A. Yoshikawa, *IEEE Trans. Nucl. Sci.*, **2008**, *55*, 2420.
7) C. Liu, Z. G. Neale, G. Cao, *Materials Today*, **2016**, *19*, 2.
8) K. Kamada, T. Yanagida, T. Endo, K. Tsutumi, M. Yoshino, J. Kataoka, Y. Usuki, Y. Fujimoto, A. Fukabori, A. Yoshikawa, *J. Cryst. Growth*, **2012**, *352*, 91.
9) M. V. Derdzyan, K. L. Ovanesyan, A. G. Petrosyan, A. Belsky, C. Dujardin, C. Pedrini, E. Auffray, P. Lecoq, M. Lucchini, K. Pauwels, *J. Cryst. Growth*, **2012**, *361*, 212.
10) A. G. Petrosyan, V. F. Popova, V. V. Gusarov, G. O. Shirinyan, C. Pedrini, P. Lecoq, *J. Cryst. Growth*, **2006**, *293*, 74.
11) S. M. Koohpayeh, D. Fort, J. S. Abell, *Prog. Cryst. Growth Charact. Mater.*, **2008**, *54*, 121.
12) M. Higuchi, K. Kodaira, *Mater. Res. Bull.*, **1994**, *29*, 545.
13) M. M. Hossain, S. Watauchi, M. Nagao, I. Tanaka, *Cryst. Growth Des.*, **2014**, *14*, 5117-5121.
14) S. Watauchi, M. Suzuki, M. Nagao, I. Tanaka, *J. Cryst. Growth*, **2018**, *496-497*, 69.
15) M. A. R. Sarker, S. Watauchi, M. Nagao, T. Watanabe, I. Shindo, I. Tanaka, *J. Cryst. Growth*, **2010**, *312*, 2008.
16) M. A. R. Sarker, S. Watauchi, M. Nagao, T. Watanabe, I. Shindo, I. Tanaka, *J. Cryst. Growth*, **2011**, *317*, 135.
17) S. Watauchi, M.A.R Sarker, M. Nagao, I. Tanaka, T. Watanabe, I. Shindo, *J. Cryst. Growth*, **2012**, *360*, 105.
18) M. M. Hossain, S. Watauchi, M. Nagao, I. Tanaka, *J. Cryst. Growth*, **2016**, *433*, 24.
19) K. Kitamura, S. Kimura, K. Watanabe, *J. Cryst. Growth*, **1982**, *57*, 475.
20) K. Kitamura, S. Kimura, S. Hosoya, *J. Cryst. Growth*, **1980**, *48*, 469.
21) S. Watauchi, I. Tanaka, K. Hayashi, M. Hirano, H. Hosono, *J. Cryst. Growth*, **2002**, *237-239*, 801.
22) M. M. Hossain, S. Watauchi, M. Nagao, I. Tanaka, *J. Cryst. Growth*, **2017**, *459*, 105.